Hybrid modeling of the mega-tsunami runup in Lituya Bay after half a century

Robert Weiss,[1] Hermann M. Fritz,[2] and Kai Wünnemann[3]

Received 20 February 2009; revised 1 April 2009; accepted 10 April 2009; published 9 May 2009.

[1] The largest mega-tsunami dates back half a century to 10 July 1958, when almost unnoticed by the general public, an earthquake of M_w 8.3 at the Fairweather Fault triggered a rockslide into Lituya Bay. The rockslide impact generated a giant tsunami at the head of Lituya Bay resulting in an unprecedented tsunami runup of 524 m on a spur ridge in direct prolongation of the slide axis. A forest trim line and erosion down to bedrock mark the largest runup in recorded history. While these observations have not been challenged directly, they have been largely ignored in hazard mitigation studies, because of the difficulties of even posing – much less solving – a well-defined physical problem for investigation. We study the mega-tsunami runup with a hybrid modeling approach applying physical and numerical models of slide processes of deformable bodies into a U-shaped trench similar to the geometry found at Lituya Bay. **Citation:** Weiss, R., H. M. Fritz, and K. Wünnemann (2009), Hybrid modeling of the mega-tsunami runup in Lituya Bay after half a century, *Geophys. Res. Lett.*, *36*, L09602, doi:10.1029/2009GL037814.

1. Geographical and Geological Setting

[2] Lituya Bay is a T-shaped tidal inlet cutting through coastal lowlands and foothills of the Fairweather Range on the Pacific south coast of Alaska (Figure 1). The bay fills and slightly overflows a glacially carved depression with characteristic submarine contours [*Miller*, 1960]. The pronounced U-shaped trench with steep side walls and a broad flat seafloor is 12 km long, up to 3.3 km wide and 220 m deep. The Gilbert and Crillon inlets at the head of the bay are part of a great trench that extends to the northwest and southeast as a topographic expression of the Fairweather transform fault.

[3] Giant waves have likely occurred in Lituya Bay at least five times in the past two centuries as a result of the interplay between the geological and climatic setting [*Miller*, 1960]. Evidence of extreme wave-runup heights in 1853 or 1854, 1936 and 1958 have each been identified by sharp trim lines of chopped trees to elevations above 100 m. Two additional giant waves may have occurred in 1874 and 1899. These are not typical landslide waves as often occur in other Alaskan fjords [*Plafker*, 1969; *Synolakis et al.*, 2002].

[4] On 10 July 1958 beginning at 6:16 UTC intense shaking from an M_w 8.3 earthquake [*Tocher and Miller*, 1959] caused 6.4 m horizontal and 1 m vertical tectonic movement. An estimated rockslide volume of about 30×10^6 m^3 was released on the northeast wall of the Gilbert Inlet up to an elevation of 915 m on a slope averaging 40 degrees (Figure 2). The slide material was composed of amphibole and biotite schist. The initial slide geometry is assumed to be a prism spanning 730 m to 915 m in width and a thickness of 92 m normal to the slope. The lower extent of the initial landslide position remains undefined. The slide length was estimated to 970 m with a center of gravity at 610 m elevation [*Slingerland and Voight*, 1979; *Miller*, 1960]. The landslide sheared off and washed away up to 400 m of ice from the Lituya Glacier front resulting in a vertical ice wall perpendicular to Gilbert Inlet. The landslide impact generated tsunami produced unprecedented runup heights of 524 m on a headland in slide axis prolongation and 208 m on the south shore of Lituya Bay. The only other two landslide tsunami events known to produce runup heights exceeding 200 m are Vajont reservoir in 1963 [*Müller*, 1964, 1968] and Spirit Lake in 1980 [*Voight et al.*, 1981, 1983].

2. Experiments

[5] Based on generalized Froude similarity, *Fritz et al.* [2001] built a 2D physical model of the Gilbert inlet scaled at 1:675. The prototype unit volume of the slide was determined to $\sim 37.2 \times 10^3$ m^3/m based on a volume of 30.6×10^6 m^3 spread over an average width of 823 m. The bathymetry and topography are simplified in the laboratory by headlands with slope angles (α and β) of 45 degrees and maximum uniform water depth (h) of 122 m at prototype scale. The short tsunami propagation distance combined with the confining wall formed by the Lituya Glacier may justify a simplified two-dimensional approach given the limited space for 3D spreading (Figure 2) [*Fritz et al.*, 2009].

[6] The Lituya Bay rockslide was modeled with an artificial granular material (PP-$BaSO_4$) matching the density of the prototype schist. Given the unit volume, the slide mass per unit width is $m' = 98.5 \times 10^3$t/m. The slide granulate, initially contained in the slide box, is accelerated by a pneumatic landslide generator to control landslide dynamics and impact characteristics. Two laser-distance sensors measure granular slide profiles before impact. A laser-based digital PIV-system provides instantaneous velocity vector fields in the slide impact and runup areas providing insight into the kinematics of wave generation and

[1]Department of Geology and Geophysics, Texas A&M University, College Station, Texas, USA.
[2]Civil and Environmental Engineering, Georgia Institute of Technology, Savannah, Georgia, USA.
[3]Museum für Naturkunde, Leibniz Institute, Humboldt University of Berlin, Berlin, Germany.

0094-8276/09/2009GL037814

Figure 1. Lituya Bay, Alaska satellite image (August 2001, Landsat) with superimposed 1958 landslide scar at the head of the bay and forest trimline of tsunami runup after *Miller* [1960]. Note the forest destruction to a maximum runup elevation of 524 m on a spur ridge and a maximum inundation distance of 1100 m from high-tide shoreline at Fish Lake.

runup (Figure 3) [*Fritz et al.*, 2003]. A capacitive wave gauge is installed at a distance of 885 m from the slide impact along with two runup gauges on the headland. In the physical model, the slide mass is accelerated up to a prototype impact velocity v of 110 m/s, which corresponds to an estimated free-fall velocity with the centroid situated at 610 m elevation [*Law and Brebner*, 1968; *Noda*, 1970], resulting in an impact slide Froude number $F = v/(gh)^{0.5} = 3.18$.

3. Hydrocode Modeling

[7] We adapted the multi-material hydrocode iSALE (Impact Simplified Arbitrary Lagrangian Eulerian) [e.g., *Wünnemann et al.*, 2006, and references therein] to simulate the Lituya Bay rockslide and tsunami. iSALE is a multi-material, finite-difference hydrocode for simulating fluid flows and deformations of solid bodies at subsonic and supersonic speeds. A full description of the code is beyond the scope of this paper and we refer to the manual of the original code by *Amsden et al.* [1980] and more general literature on hydrocode modeling, see, e.g., *Pierazzo and Collins* [2004], *Benson* [1992] and *Anderson* [1987].

[8] The basic approach of the algorithm used in iSALE is to deform a regular grid of computational cells in a *Lagrangian step* according to the velocity field computed at the grid nodes. The deformed grid is then remapped (at the end of each time step) onto the original orthogonal mesh by advecting cell-based quantities (density, energy, momentum) through cell boundaries. The overall method applied then corresponds to an *Eulerian* solution scheme, where the computational mesh is fixed in space and material flows through it. To accurately simulate the movement of more than one material in an *Eulerian* mesh, where material is fluxed through a stationary mesh, requires the tracking of interfaces between two materials within one cell (mixed cell). For general information on interface tracking techniques see, e.g., *Benson* [2002].

[9] The equations for conservation for mass, momentum, and energy are solved by using a first-order upwind (full donor cell) advection scheme. The material is treated compressible, therefore an equation of state (EoS) is required to compute pressure as a function of density and internal energy. Because compression is small (velocities are much smaller than the speed of sound in the material), we used, for simplicity, the Tillotson EoS [*Tillotson*, 1962] for water, and granite for the slidebody and slope (for EoS parameters see, e.g., *Melosh* [1989]).

[10] To calculate the deviatoric stress tensor and its effect on the velocity field, iSALE employs a deviatoric stress model similar to that described by *Collins et al.* [2004] and *Ivanov et al.* [1997]. In each time step, the second invariant of the stress tensor in a cell is compared to the yield strength of the material. Where the invariant exceeds the yield envelope stresses are modified accordingly to meet the yield strength of the material again.

[11] The yield strength in the slide body is calculated by a simple *Drucker-Prager* strength model with zero cohesion, in which the yield strength Y is a linear function of pressure

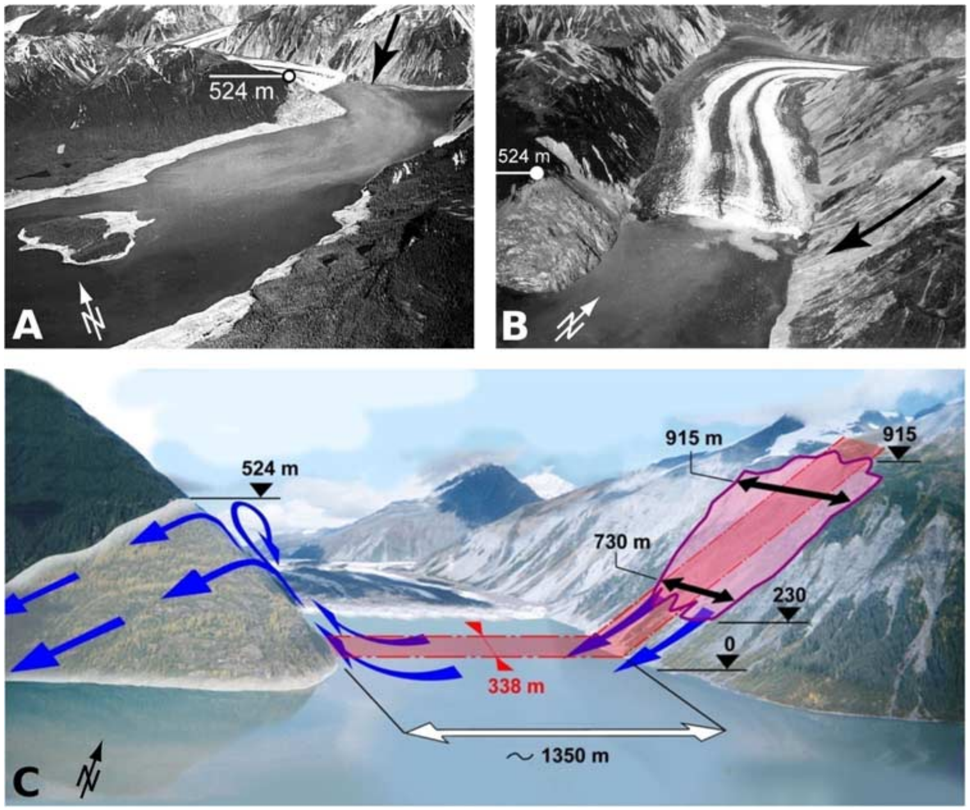

Figure 2. Trimlines carved by tsunami in 1958: (a) NE_view of Lituya Bay from Cenotaph Island to Gilbert Inlet with landslide scar at the head of the bay and trimlines of destructed forest with 524 m runup on spur ridge. (b) NW_view of Gilbert Inlet with landslide scar, post_event Lituya Glacier front, forest destruction and soil erosion down to bedrock (Photos: courtesy of USGS). (c) Gilbert Inlet illustration showing landslide dimensions, impact site and tsunami runup to 524 m on spur ridge directly opposite to landslide impact. Direction of view is north and the front of Lituya Glacier is set to 1958 post slide position. Illustration background is synthesized from two aerial photos recorded in 1997.

p: $Y = C + \mu p$ (μ is coefficient of internal friction and $C = 0$ is cohesion). A *Drucker-Prager* material model appropriately represents the behavior of granular material such as gravel. For the rigid slopes and the basement we assumed an infinite cohesion to avoid any movement or deformation during the slide process. Water behaves like an inviscid fluid in our model.

[12] iSALE is validated against experimental studies of hypervelocity impacts and other hydrocodes [*Pierazzo et al.*, 2008] and used successfully in modeling of meteorite impact wave generation studies [*Weiss et al.*, 2006; *Wünnemann et al.*, 2007].

[13] The general model setup is described in detail by, e.g., *Wünnemann and Lange* [2002]. iSALE supports two different geometries: a Cartesian and a Cylindrical grid. For two-dimensional computations, without radial spreading of waves, the Cartesian coordinate system is used for the modeling on prototype scale (Figure 2). Assuming a constant volume of the slide body as in the laboratory experiments, three parameters, (i) initial velocity, (ii) density, and (iii) friction, constrain the wave generation. In order to match the experimental data, an initial velocity is introduced to meet the impact velocity of 110 m/s. The grains have a density of $\rho_g = 2640$ kg/m^3, but the slide impact density is set to the bulk density of the granular material, $\rho_s = 1610$ kg/m^3, by introducing a porosity of 39%. iSALE supports treatment of porosity as a function of volumetric strain [*Wünnemann et al.*, 2006]; however, in our models we kept the porosity constant at 39% during the slide process. Measured internal friction coefficient of the granular material range between 0.9–1.0 [*Fritz*, 2002]. The friction coefficient of the slide body in the model was set to $\mu = 0.4$ which corresponds to the bed friction coefficient between the slope and the slide body in the experiments. In the current version of iSALE it is possible to use different internal friction coefficients for the slope and the slide body, but the code does not allow for specifying friction coefficients for interfaces between materials, e.g., slope and slide. For the dynamics of the slide body it appears to be more important to match the bed friction. Although the too small internal friction coefficient of the slide body may enhance deformation of the body during slide and impact into the water.

4. Results

[14] The time series of free surface elevations recorded by the wave gauge documents the generation of a single impulse wave which reaches its maximum 16 s after the impact at 152 m, propagating towards the headland (Figure 4). The second crest after 48 s represents the wave reflection from the head wall. Various empirical and theoretical predictive relationships for the landslide-generated tsunami amplitude

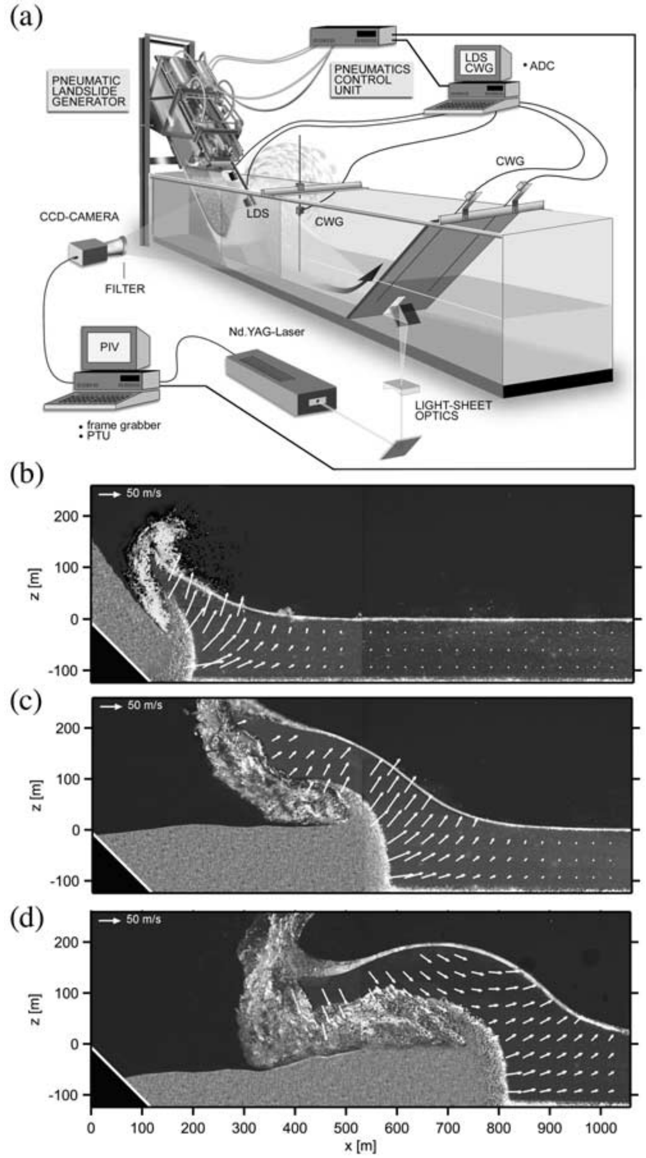

Figure 3. Landslide tsunami experiment: (a) Experimental setup with pneumatic installation and measurement systems: Laser distance sensors (LDS), capacitance wave gages (CWG) and particle image velocimetry (PIV). (b–d) PIV velocity vector plot sequence of two synchronized granular slide impact experiments with juxtaposed areas of view and up_scaled parameters: Froude number F = 3.18, impact velocity v = 110 m/s, mass per unit width m' = 95.5×103 t/m′, water depth h = 122 m, slope angles $\alpha = \beta = 45°$, time increment 5.19 s with the first image at t = 2.49 s after impact. Highlighted is the flow separation on the back of the landslide and the formation of an impact crater [*Fritz et al.*, 2001].

were compared with the Lituya Bay benchmark experiment [*Fritz et al.*, 2004]. The solutions by *Hall and Watts* [1953] and *Synolakis* [1986, 1987] for solitary wave runup on impermeable slopes match the experimentally measured wave runup and the observed elevation of forest destruction in Lituya Bay with predictions of R = 526 m and R = 493 m based on experimentally measured incident wave parameters H = 162 m and h = 122 m [*Fritz et al.*, 2001]. This confirms the 160 m wave height by *Slingerland and Voight* [1979] inferred from back calculation from the runup. The wave height of the measured solitary-like wave exceeds solitary wave breaking criteria H/h = 0.83 [*Tanaka*, 1986]. Consequently, the leading wave does collapse into a bore in experiments without the headland providing sufficient propagation distance for wave evolution [*Fritz et al.*, 2003]. However the solitary-like wave in Gilbert Inlet does not extensively break due to the short propagation distance and the steep headland slope [*Jensen et al.*, 2003].

[15] The slide body deforms in the numerical simulation as it moves down the slope and is shown just before impacting the water in Figure 4b (t = 4 s). The maximum of the first peak in time series of Figure 4g corresponds to Figure 4c (t = 19 s). Shortly after the maximum wave height passes the tide gauge at 885 m from the headland of the wave impact, partial breaking of the generated wave is indicated in Figure 4d. The water mass runup on the headland slope with subsequent resurge creates the second crest shown in Figure 4e (t = 53 s). Severe wave breaking can be observed near the hillslope slope. In Figure 4f, the second maximum passed and the water mass moved the slide body moved to the west. Given the complexity of the water movement and the nonlinearity of the generated waves, time series of the water elevation help to evaluate generated waves in laboratory experiments and in numerical models, but also serve as important validation for numerical models. The agreement between experimental and modeled data for the tide gauge in 885 m distance from the impact slope is remarkable for both amplitude and phase (Figure 4g). The maximum amplitude is A = 152 m occurs approximately 16 s after the impact into the water. The maximum runup of 518m modeled with iSALE is remarkably close to both observed and experimentally measured runup heights of about 524 m.

5. Conclusion

[16] We studied the 1958 Lituya Bay rockslide and tsunami numerically and by analog modeling in the laboratory, the latter at a scale of 1:675 using a unique pneumatic landslide tsunami generator to control the slide impact characteristics. To match the runup of 524 m, the slide volume estimated by *Miller* [1960] was accelerated to an impact velocity of 110m/s. The impact formed a large air cavity and a highly nonlinear wave. Using the geometry of the physical model at prototype scale, iSALE computed the detailed evolution of the coupled free surface and slide deformations. Comparisons between experimental and modeling results show an excellent agreement, indicating that all dominant processes are approximated adequately raising the possibility of more advanced hazard mitigation studies in the region. After half a century, the numerous landslide deposits in Lituya Bay still remain to be mapped to establish a baseline bathymetry prior to any possible future landslide tsunami in Lituya Bay. With such a bathymetry, the Lituya Bay rockslide and tsunami as well as other extreme events can be understood with the help of the same hybrid approach consisting of three-dimensional

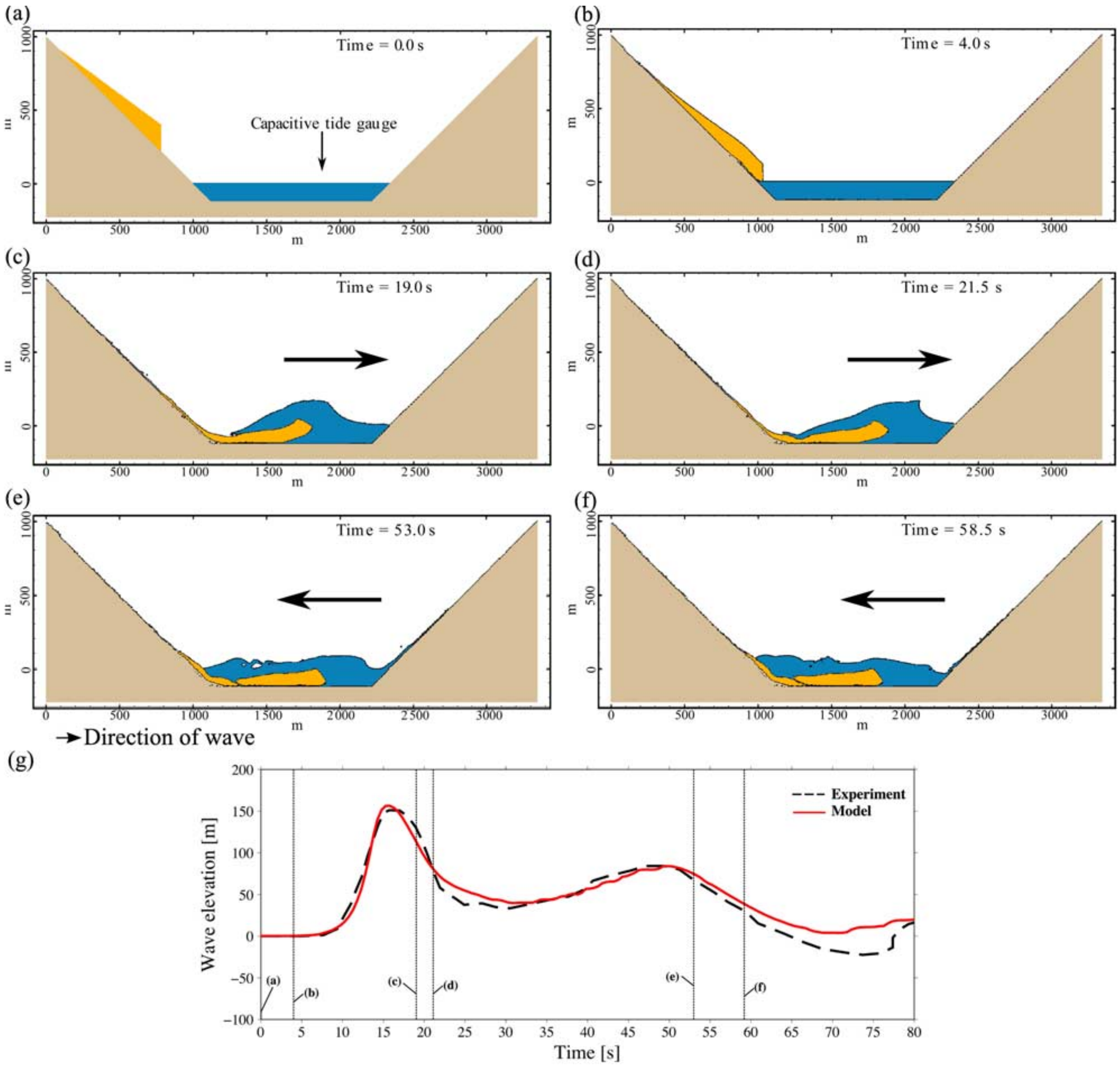

Figure 4. (a–f) Snapshots illustrating the direction of water movement associated with the maxima in the time series. (g) Tsunami wave gauge record at location x = 885 m Dashed lines indicate instances in Figures 4a–4f.

experiments [*Fritz et al.*, 2009] and three-dimensional modeling with iSALE-3D.

[17] **Acknowledgments.** H.F. was supported by the National Science Foundation under grant CMMI-0421090. Any opinions, findings, and conclusions or recommendations expressed herein are those of the author(s) and do not necessarily reflect the views of the National Science Foundation. The two-dimensional experiments conducted at VAW (ETH Zurich) were supported by the Swiss National Science Foundation under grant 2100-050586.97. K.W. was supported by DFG grant WU 355/5-2 and is grateful for the financial support by the NOAA Center for Tsunami Research (NCTR), PMEL. R.W. thanks management and personnel of the NOAA Center for Tsunami Research and the Pacific Marine Environmental laboratory for their support and guidance during his tenure at NCTR.

References

Amsden, A. A., H. M. Ruppel, and C. W. Hirt (1980), SALE: A simplified ALE computer program for fluid flows at all speeds, *Rep. LA-8095*, Los Alamos Natl. Lab., Los Alamos, N. M.

Anderson, C. E., Jr. (1987), An overview of the theory of hydrocodes, *Int. J. Impact Eng.*, *5*, 33–59.

Benson, D. J. (1992), Computational methods in Lagrangian and Eulerian hydrocodes, *Comput. Meteorol. Appl. Mech. Eng.*, *99*, 235–394.

Benson, D. J. (2002), Volume of fluid interface reconstruction methods for multi-material problems, *Appl. Mech. Rev.*, *55*, 151–165.

Collins, G. S., H. J. Melosh, and B. A. Ivanov (2004), Modeling damage and deformation in impact simulations, *Meteorit. Planet. Sci.*, *39*, 217–231.

Fritz, H. M. (2002), Initial phase of landslide generated impulse waves. Ph.D. thesis ETH-No. 14871, Swiss Federal Institute of Technology, ETH Zürich, Switzerland.

Fritz, H. M., W. H. Hager, and H.-E. Minor (2001), Lituya Bay case: Rockslide impact and wave runup, *Sci. Tsunami Hazards*, *19*, 3–22.

Fritz, H. M., W. H. Hager, and H.-E. Minor (2003), Landslide generated impulse waves: Part 1. Instantaneous flow fields, *Exp. Fluids*, *35*, 505–519.

Fritz, H. M., W. H. Hager, and H.-E. Minor (2004), Near field characteristics of landslide generated impulse waves, *J. Waterw. Port Coastal Ocean Eng.*, *130*, 287–302.

Fritz, H. M., F. Mohammed, and J. Yoo (2009), Lituya Bay landslide impact generated mega-tsunami 50th anniversary, *Pure Appl. Geophys.*, *166*, 153–175, doi:10.1007/s00024-008-0435-4.

Hall, J. V., Jr., and G. M. Watts (1953), Laboratory investigation of the vertical rise of solitary waves on impermeable slopes, *Tech. Memo. 33*, U.S. Army Corps of Eng., Washington, D. C.

Ivanov, B. A., D. Deniem, and G. Neukum (1997), Implementation of dynamic strength models into 2D hydrocodes: Applications for atmospheric breakup and impact cratering, *Int. J. Impact Eng.*, *20*, 411–430.

Jensen, A., G. K. Pedersen, and D. J. Wood (2003), An experimental study of wave runup at a steep beach, *J. Fluid Mech.*, *486*, 161–188, doi:10.1017/S0022112003004543.

Law, L., and A. Brebner (1968), On water waves generated by landslides, in *Proceedings of the Third Australasian Conference on Hydraulics and Fluid Mechanics*, pp. 155–159, Inst. of Eng., Sydney, N. S. W., Australia.

Melosh, H. J. (1989), *Impact Cratering: A Geologic Process*, *Oxford Monogr. Geol. Geophys.*, vol. 11, Oxford Univ. Press, New York.

Miller, D. J. (1960), Giant waves in Lituya Bay, Alaska, *U. S. Geol. Surv. Prof. Pap.*, *354-C*.

Müller, L. (1964), The rock slide in the Vajont Valley, *Rock Mech. Eng. Geol.*, *2*, 148–212.

Müller, L. (1968), New considerations on the Vajont slide, *Rock Mech. Eng. Geol.*, *6*, 1–91.

Noda, E. (1970), Water waves generated by landslides, *J. Waterw. Harbors Coastal Eng. Div. Am. Soc. Civ. Eng.*, *96*, 835–855.

Plafker, G. (1969), Tectonics of the March 27, 1964, Alaska earthquake, *U. S. Geol. Surv. Prof. Pap.*, *543-I*.

Pierazzo, E., and G. S. Collins (2004), A brief introduction to hydrocode modelling of impact cratering, in *Impact Studies: Cratering in Marine Environments and on Ice*, edited by D. Henning et al., p. 323, Springer, New York.

Pierazzo, E., et al. (2008), Validation of numerical codes for impact and explosion cratering: Impacts on strengthless and metal targets, *Meteorit. Planet. Sci.*, *43*, 1917–1939.

Slingerland, R. L., and B. Voight (1979), Occurrences, properties and predictive models of landslide-generated impulse waves, in *Rockslides and Avalanches*, *Dev. Geotech. Eng.*, vol. 14A–14B, edited by B. Voight, p. 317, Elsevier, Amsterdam.

Synolakis, C. E. (1986), The runup of long waves, Ph.D. thesis, Calif. Inst. of Technol, Pasadena.

Synolakis, C. E. (1987), The runup of solitary waves, *J. Fluid Mech.*, *185*, 523–545.

Synolakis, C. E., A. C. Yalciner, J. C. Borrero, and G. Plafker (2002), Modeling of the November 3, 1994 Skagway, Alaska tsunami, in *Solutions to Coastal Disasters 2008 Tsunamis*, edited by L. Wallendorf and L. Ewing, pp. 915–927, Am. Soc. of Civ. Eng., Reston, Va.

Tanaka, M. (1986), The stability of Solitary waves, *Phys. Fluids*, *29*, 650–655.

Tillotson, J. H. (1962), Metallic equations of state for hypervelocity impacts, *Gen. At. Rep. GA-3216*, Gen. At. Div. of Gen. Dyn., San Diego, Calif.

Tocher, D., and D. J. Miller (1959), Field observations on effects of Alaskan earthquake of 10 July, 1958, *Science*, *129*, 394–395.

Voight, B., H. Glicken, R. J. Janda, and P. M. Douglass (1981), *Catastrophic rockslide-avalanche of May 18: The 1980 eruptions of Mount St. Helens, Washington*, edited by P. W. Lipman and D. R. Mullineaux, *U. S. Geol. Surv. Prof. Pap.*, vol. 1250, pp. 347–377.

Voight, B., R. J. Janda, H. Glicken, and P. M. Douglass (1983), Nature and mechanics of the Mount St. Helens rockslide-avalanche of 18 May 1980, *Géotechnique*, *33*, 243–273.

Weiss, R., K. Wünnemann, and H. Bahlburg (2006), Numerical modelling of generation, propagation and run-up of tsunamis caused by oceanic impacts: Model strategy and technical solutions, *Geophys. J. Int.*, *167*, 77–88.

Wünnemann, K., and M. A. Lange (2002), Numerical modeling of impact-induced modifications of the deep-sea floor, *Deep Sea Res., Part II*, *49*, 669–981.

Wünnemann, K., G. S. Collins, and H. J. Melosh (2006), A strain-based porosity model for use in hydrocode simulations of impacts and implications for transient crater growth in porous targets, *Icarus*, *180*, 514–527.

Wünnemann, K., R. Weiss, and K. Hofmann (2007), Characteristic of oceanic impact induced large water waves–reevaluation of the tsunami hazard, *Meteorit. Planet. Sci.*, *42*, 1893–1903.

H. M. Fritz, Civil and Environmental Engineering, Georgia Institute of Technology, Savannah, GA 31407, USA. (fritz@gatech.edu)

R. Weiss, Department of Geology and Geophysics, Texas A&M University, College Station, TX 77843, USA. (weiszr@tamu.edu)

K. Wünnemann, Museum für Naturkund, Leibniz Institute, Humboldt University of Berlin, Invalidenstr. 43, D-10115 Berlin, Germany. (kai.wuennemann@museum.hu-berlin.de)